Rev. Adv. Mater. Sci. 39 (2014) 54-60

EFFECT OF COOPERATIVE GRAIN BOUNDARY SLIDING AND NANOGRAIN NUCLEATION ON CRACK GROWTH IN NANOCRYSTALLINE MATERIALS AND METAL-CERAMIC NANOCOMPOSITES

I.A. Ovid'ko[1,2,3] and A.G. Sheinerman[1,2,3]

[1]St. Petersburg State Polytechnical University, St. Petersburg 195251, Russia
[2]Institute of Problems of Mechanical Engineering, Russian Academy of Sciences, Bolshoj 61, Vasilievskii Ostrov, St. Petersburg 199178, Russia
[3]Department of Mathematics and Mechanics, St. Petersburg State University, St. Petersburg 198504, Russia

Received: September 29, 2014

Abstract. A new mechanism of fracture toughness enhancement in nanocrystalline materials and metal-ceramic nanocomposites is suggested. The mechanism represents the cooperative grain boundary sliding and nanograin nucleation (CGBSNN) process near the tips of growing cracks. It is shown that this mechanism can increase the critical stress intensity factor for crack growth in nanocrystalline and nanocomposite materials at least by a factor of 2 to 3 (or even more in some cases), as compared to the case of pure brittle fracture, and thus considerably enhances the fracture toughness of such materials.

1. INTRODUCTION

Single-phase nanocrystalline materials (NMs) and nanocrystalline-matrix composites (NMCs) show excellent mechanical properties that are of high interest from both fundamental and applied viewpoints (see, e.g., original papers [1–16] and reviews [17–23]). First of all, these solids are specified by superior strength and hardness. At the same time, single-phase NMs and NMCs are often characterized by low values of ductility and fracture toughness, which severely limit their practical utility [17–23]. However, in some cases, NMs and NMCs show considerable tensile ductility at room temperature [11,17,24–26] as well as functional fracture toughness [27–31]. One of logical explanations of enhanced ductility and/or functional fracture toughness in several nanomaterials is based on the ideas that specific deformation modes operate on the nanoscale, and, in several cases, these modes are effective in providing enhanced ductility and/or toughness; for a review, see [32]. In particular, grain boundary (GB) sliding is viewed to be a GB deformation mode that often crucially contributes to plastic flow and toughness enhancement in nanocrystalline materials [17–23,33]. Recently, it has been theoretically revealed that, in nanocrystalline materials, GB sliding can cooperatively and effectively operate with other GB deformation modes, such as stress-driven GB migration [34] and stress-driven nanograin nucleation [35]. In the former case, the cooperative GB sliding and migration process has been theoretically recognized as the nanoscale deformation mode that can very effectively improve fracture toughness of a nanocrystalline specimen where it operates [36]. At the same time, the effect of another cooperative deformation mode – the cooperative GB sliding and nanograin nucleation (CGBSNN) process – on fracture toughness in nanomaterials is unclear. The main

Corresponding author: I.A. Ovid'ko, e-mail: ovidko@nano.ipme.ru

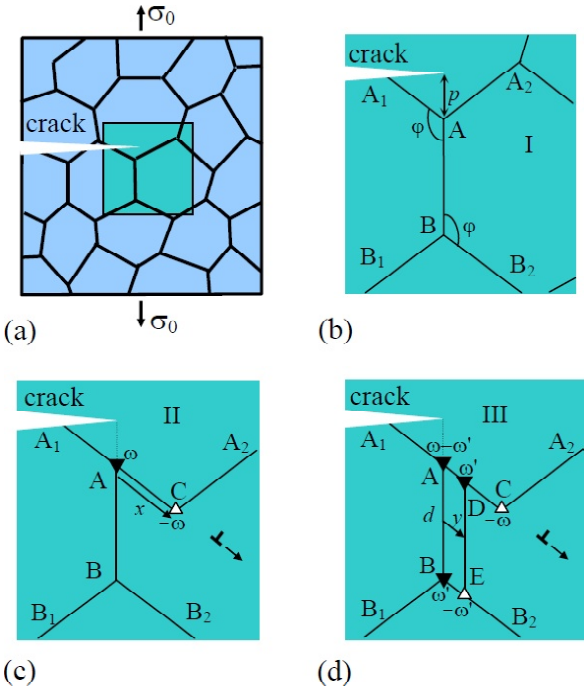

Fig. 1. Grain boundary deformation processes in nanocrystalline specimen near a crack tip. (a) General view. (b) Initial configuration I of grain boundaries. (c) Configuration II results from pure grain boundary sliding. Dipole of disclinations AC is generated due to grain boundary sliding. (d) Configuration III results from cooperative grain boundary sliding and nanograin nucleation process. Five disclinations at points A, B, C, D and E are generated due to this cooperative process.

aim of this paper is to theoretically describe the role of the CGBSNN process in hindering crack growth and estimate the effect of this process on fracture toughness in single-phase NMs and metal-ceramic nanocomposites.

2. COOPERATIVE GRAIN BOUNDARY MIGRATION AND NANOGRAIN NUCLEATION NEAR A CRACK TIP. MODEL

Let us consider the geometric features of the CGBSNN in a deformed nanocrystalline specimen containing a crack (Fig. 1). Within our model, the crack is flat, and the specimen is under a tensile load σ_0 normal to the crack plane (Fig. 1a). The applied load and high stress concentration near the crack tip can induce both GB sliding and GB splitting followed by migration of the new GB, in which case a and new nanograin nucleates near this crack tip (Fig. 1). These processes release, in part, high elastic stresses near the crack tip and thereby can slow down crack growth. It is logically assumed that the intensity of CGBSNN process and its effect on crack growth strongly increase with a decrease of the distance between the crack tip and GBs involved in this process. With this assumption, the dominant effect of the CGBSNN process on crack propagation is caused by this process in vicinity of the crack tip.

Let us consider geometry of the CGBSNN process in a nanocrystalline specimen (Fig. 1). Fig. 1a shows a two-dimensional section of a deformed nanocrystalline specimen. Within the model [35], sliding along the GB A_1A by a distance x occurs under the applied stress and transforms the initial configuration I of GBs (Fig. 1b) into configuration II (Fig. 1c). GB sliding is assumed to be accommodated, in part, by emission of lattice dislocations from triple junctions (Fig. 1c). Besides, following [37,38], GB sliding results in the formation of a dipole of wedge disclinations A and C in configuration II (Fig. 1c) characterized by strengths $\pm\omega$, whose magnitude ω is equal to the tilt misorientation of the GB (AB is assumed to be a symmetric tilt boundary). The distance between the disclinations A and C is has an arm equal to the magnitude x of the relative displacement of grains (Fig. 1c).

We further assume [35] that, in parallel with GB sliding, nanograin nucleation occurs as well. During this process, the GB AB splits into the two GB fragments: the immobile fragment (also called AB) and the mobile GB fragment DE, which, for simplicity, is supposed to be a symmetric tilt boundary. The GB fragment DE under the action of the resolved shear stress moves over the distance y from its initial position AB (Fig. 1d). Hereinafter, for simplicity, we consider the GB configuration with planar and parallel GBs AC and BE, in which case the length of the migrating GB does not change. Following [35,39,40], the splitting and migration of the GBs under consideration lead to the following transformations of the GB disclinations: (1) the disclination A characterized by the strength ω in its initial state (Fig. 1c) splits into the new disclination A with the strength $\omega - \omega'$ and the new disclination D with the strength ω' (Fig. 1d); (2) a new disclination dipole BE with disclination strengths $\pm\omega'$ is formed (Fig. 1d). In doing so, the strength ω' is equal by magnitude to the misorientation angle of the new GB DE. The area ADEB represents a new nanograin whose formation is associated with migration of the GB DE and corresponding movement of disclination dipole DE.

3. EFFECT OF COOPERATIVE GRAIN BOUNDARY MIGRATION AND NANOGRAIN NUCLEATION ON CRITICAL STRESS INTENSITY FACTOR IN NANOCRYSTALLINE SOLIDS

Now let us consider the effect of the applied tensile load and a long flat mode I crack on the CGBSNN process in a nanocrystalline specimen (Fig. 1). The specimen is supposed to be an elastically isotropic solid characterized by the shear modulus G and Poisson's ratio ν. The vertical GB is assumed to be normal to the crack growth direction and make an angle φ with the grain boundaries AA_1 and BB_2 (Fig. 1b). Let the triple junction A be distant by p from the crack tip and the length of all GBs in the initial state (Fig. 1b) be denoted as d. In order to calculate the parameters of the CGBSNN process, first, let us calculate the energy change ΔW associated with the formation of the disclination configuration shown in Fig. 1d. The energy change ΔW can be written as follows:

$$\Delta W = \sum_{j=1}^{5} W^{\Delta}(r_j,\theta_j,\omega_j) + \sum_{j=1}^{5} W^{\Delta-\sigma}(r_j,\theta_j,\omega_j) + \sum_{j=1}^{5}\sum_{k=1}^{j-1} W_{\text{int}}(r_j r_k,\theta_j,\theta_k,\omega_j,\omega_k) - A_{sl} + E_{GB}, \quad (1)$$

where (r_j,θ_j) are the coordinates of the jth disclination in the polar coordinate system with the origin at the crack tip (j = 1,2,3,4,5; see Fig. 1); ω_j is the strength of the jth disclination; $W^{\Delta}(r_j,\theta_j,\omega_j)$ is the energy of the jth disclination in the solid with a crack; $W^{\Delta-\sigma}(r_j,\theta_j,\omega_j)$ is the energy of the interaction between the jth disclination and the stress field σ_{il} induced by the applied load near the crack tip; $W_{\text{int}}(r_j, r_k, \theta_j, \theta_k, \omega_j, \omega_k)$ is the energy of the interaction between the jth and kth disclinations (in the solid with a crack), A_{sl} is the work of the stress σ_{il} done on GB sliding, which does not account for the formation of disclinations, and E_{GB} is the total change of GB energies in the course of the CGBSNN process. Values of the indices j=1,2,3,4 and 5 correspond to the disclinations at points D, C, E, B and A, respectively. The disclination strengths ω_j are given as $\omega_1 = \omega'$, $\omega_2 = -\omega$, $\omega_3 = -\omega'$, $\omega_4 = \omega'$, and $\omega_5 = \omega - \omega'$. The coordinates (r_j,θ_j) are calculated as follows:

$$r_1(y) = \left(y^2 + p^2 - 2yp\cos\varphi\right)^{1/2},$$

$$r_2(x) = \left(x^2 + p^2 - 2xp\cos\varphi\right)^{1/2},$$

$$r_3(y) = \left(y^2 + (p+d)^2 - 2y(p+d)\cos\varphi\right)^{1/2},$$

$$r_4 = p + d,\ \ r_5 = p,$$

$$\theta_1(y) = -\arccos\left(y\sin\varphi / r_1\right),$$

$$\theta_2(x) = -\arccos\left(x\sin\varphi / r_2\right),$$

$$\theta_3(y) = -\arccos\left(y\sin\varphi / r_3\right),\ \ \theta_4 = \theta_5 = -\pi/2.$$

In Eq. (1), we neglected the resistance to GB sliding related to the "friction" of the grain boundary AA_1. The energy term $W^{\Delta}(r,\theta,\omega)$ appearing in formula (1) can be written as $W^{\Delta}(r,\theta,\omega) = [G\omega^2 d^2 h(r/d)]/[4\pi(1-\nu)]$, where $h(r/d)$ is a known function [41]. Similarly, the energy term $W_{\text{int}}(r_j,r_k,\theta_j,\theta_k,\omega_j,\omega_k)$ can be written as follows: $W_{\text{int}}(r_j,r_k,\theta_j,\theta_k,\omega_j,\omega_k) = [G\times\omega_j\omega_k d^2 g(r_j/d, r_k/d, \theta_j,\theta_k)]/[4\pi(1-\nu)]$, where $g(r_j/d, r_k/d, \theta_j,\theta_k)$ is also a known function [6]. The energy term $W^{\Delta-\sigma}(r,\theta,\omega)$ is given as [36]: ???

$$W^{\Delta-\sigma}(r,\theta,\omega) = \frac{4\omega K_I^{\sigma} r^{3/2}\cos^3(\theta/2)}{3\sqrt{2\pi}}, \quad (2)$$

The work A_{sl} of the stress σ_{il} done on GB sliding is calculated as the work of the stress σ_{il} necessary to transfer a dislocation with the Burgers vector magnitude x (equal to the length of GB sliding) across a grain boundary AA_1 of length d [36]. In doing so, one finds:

$$A_{sl} = -\frac{xK_I^{\sigma}}{2\sqrt{2\pi}} \times \int_0^d \frac{\sin\theta_2(x')\cos^2\left(3\theta_2(x')/2 + 2\varphi\right)}{\sqrt{r_2(x')}}\,dx'. \quad (3)$$

where K_I^{σ} is the stress intensity factor associated with the applied load σ_0.

Finally, the energy E_{GB} incorporates the energy of the new GB DE, the energy of the new GB fragment AC, and the energy variation of the GB AB associated with the change of its misorientation. For simplicity, we assume that the GBs A_1A and DE as well as the GB AB (both prior to and after its splitting) represent high-angle GBs whose misorientation angles are far from those of special GBs. With this assumption, in a first approximation, we will think that the specific energies of all these GBs do not depend on their misorientation angles and are approximately the same. Then we have: $E_{GB} \approx \gamma_{GB}(d + x)$, where γ_{GB} is the typical specific GB energy.

Thus, we have obtained appropriate expressions for all the energy terms appearing in Eq. (1) for the

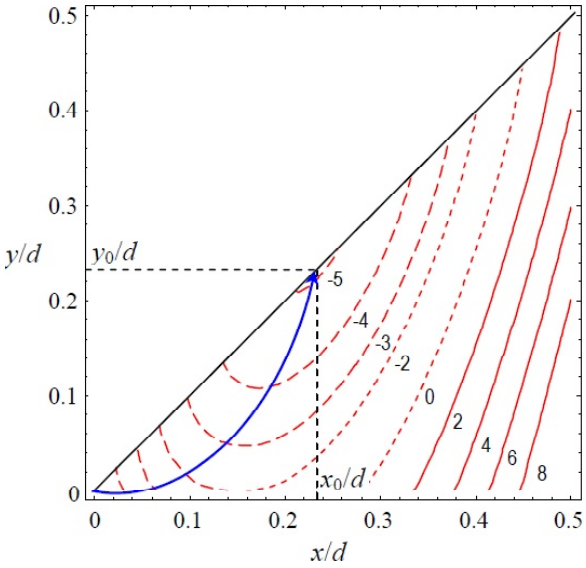

Fig. 2. Contour map of the energy change ΔW associated with the cooperative grain boundary sliding and nanograin nucleation process (near the tip of a large mode I crack in nanocrystalline Ni) in the coordinate space (x/d, y/d). The energy ΔW is given in units of 10^{-8} J/m.

total energy ΔW. With these formulas, we calculated the contour maps ΔW (x/d, y/d) (Fig. 2), in the situation with nanocrystalline Ni and $K_I^{\sigma} = K_{IC}^{br}$. Here $K_{IC}^{br} = \sqrt{4G\gamma/(1-\nu)}$ is the critical value of the stress intensity factor in the absence of disclinations (that is, in the case of brittle fracture) and γ is the specific surface energy. In plotting Fig. 3, we used the following typical values of parameters of nanocrystalline Ni and its structure: G = 76 GPa, ν = 0.31, γ = 2 J/m^2 [42], $\varphi = 2\pi/3$, d = 15 nm, $p = d$, and ω = 30°. The curve with an arrow in Fig. 3 shows the possible path of the system evolution. As it follows from Fig. 3, the minimum of ΔW (x/d, y/d) corresponds to some equilibrium values $x = x_0$ and $y = y_0$ of the lengths of sliding along the GB A_1A and migration of the new GB DE, respectively.

We now consider the effect of the disclination configuration, resulting from the CGBSNN process, on the fracture toughness of a nanocrystalline solid. To do so, we will use the standard crack growth criterion [43] based on the balance between the driving force related to a decrease in the elastic energy and the hampering force related to the formation of new free surfaces during crack growth. In the examined case of the plane strain state, this criterion is given [43] by

$$\frac{1-\nu}{2G}\left(K_I^2 + K_{II}^2\right) = 2\gamma, \qquad (4)$$

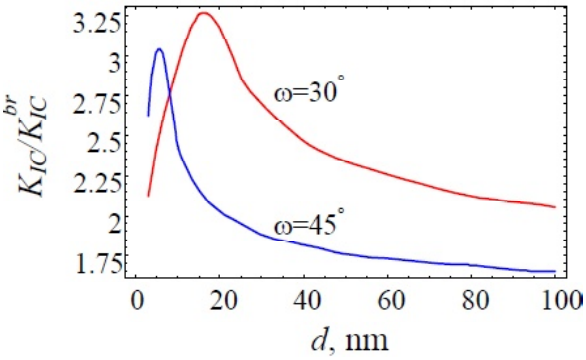

Fig. 3. Normalized critical stress intensity factor K_{IC}/K_{IC}^{br} vs grain size d for nanocrystalline Ni.

where K_I (mode I) and K_{II} (mode II) are the stress intensity factors for normal (to crack plane) and shear loading, respectively. In the considered situation where the crack growth direction is perpendicular to the direction of the external load, the coefficients K_I and K_{II} are given by the expressions

$$K_I = K_I^{\sigma} + k_I^q, \quad K_{II} = k_{II}^q, \qquad (5)$$

where k_I^q and k_{II}^q are the stress intensity factors related to the internal stresses created by the disclinations located near the crack tip (Fig. 1).

Within the above macroscopic mechanical description, the effect of the local plastic flow – the CGBSNN process resulting in the formation of wedge disclinations – on crack growth can be accounted for through the introduction of the critical stress intensity factor K_{IC}. In this case, the crack is considered as that propagating under the action of the tensile load perpendicular to the crack growth direction, while the presence of the disclinations simply changes the value of K_{IC} corresponding to the case of brittle crack propagation. In these circumstances, the critical condition for the crack growth can be represented as (e.g., [44]): $K_I^{\sigma} = K_{IC}$.

With substitution of Eq. (5) into Eq. (4) and the use of the critical condition $K_I^{\sigma} = K_{IC}$, one finds the following expression for K_{IC} [36,41]:

$$K_{IC} = \sqrt{\left(K_{IC}^{br}\right)^2 - \left(k_{IIC}^q\right)^2} - k_{IC}^q. \qquad (6)$$

The quantities in Eq. (6) are defined as follows: $K_{IC}^{br} = \sqrt{4G\gamma/(1-\nu)}$, as above, $k_{IIC}^q = k_{II}^q\big|_{K_I^{\sigma}=K_{IC}}$, and $k_{IC}^q = k_I^q\big|_{K_I^{\sigma}=K_{IC}}$. It should be noted that the quantities k_{IIC}^q and k_{IC}^q depend on K_{IC}, and, thus, Eq. (6) provides the appropriate formula for the determination of K_{IC}.

The quantities k_I^q and k_{II}^q appearing in the above expression are given [36,41] by the following rela-

tions: $k_I^q = G\sqrt{d}\, f_1(x,y)/[2\sqrt{2\pi}(1-\nu)]$ and $k_{II}^q = G\sqrt{d}\, f_2(x,y)/[2\sqrt{2\pi}(1-\nu)]$, , where

$$f_1(x,y) = \sum_{k=1}^{5} \omega_k \sqrt{r_k/d}\left[3\cos(\theta_k/2) + \cos(3\theta_k/2)\right],$$
$$f_2(x,y) = \sum_{k=1}^{5} \omega_k \sqrt{r_k/d}\left[\sin(\theta_k/2) + \sin(3\theta_k/2)\right]. \quad (7)$$

Using the above expressions, one can numerically solve Eq. (6) for K_{IC} in the following way. For a preset value of K_I^σ, one calculates the energy change ΔW and the equilibrium GB migration lengths x_0 and y_0 that correspond to a minimum of ΔW. Substituting the obtained values of x_0 and y_0 into Eqs. (7), we deduce the values of k_{IC}^q and k_{IIC}^q. Then we compute the quantities k_{IC}^q and k_{IIC}^q with the assumption that $K_I^\sigma = K_{IC}$. On the next step, we calculate K_{IC} using Eq. (6) and estimate the difference between the so obtained value of K_{IC} and the value of K_I^σ. Then we vary the preset value of K_I^σ and repeat the above procedure until the value of K_{IC} (given by Eq. (6)) becomes equal to the value of K_I^σ with sufficient accuracy.

In order to estimate the effect of the disclinations produced by the CGBSNN process (Fig. 1) on crack growth, one should compare the critical stress intensity factor K_{IC} with the quantity K_{IC}^{br}. To do so, we have calculated the ratio K_{IC}/K_{IC}^{br} in the case of nanocrystalline Ni, for $\gamma_{GB} = 0.866$ J/m^2 [45] and various values of ω. The dependences of K_{IC}/K_{IC}^{br} on grain size d are presented in Fig. 3 at $p = d$, for $\omega = 30°$ and 45°. Fig. 3 demonstrates that the CGBSNN process can increase K_{IC} by two to three times compared to the case of brittle fracture. Also, Fig. 3 demonstrates that, as the grain size increases from 3 to 100 nm, the ratio K_{IC}/K_{IC}^{br} first increases and then decreases. The maximum values of K_{IC}/K_{IC}^{br} correspond to grain sizes of 15 and 5 nm, for $\omega = 30°$ and 45°, respectively. In the corresponding ranges of grain sizes exceeding these values (15 and 5 nm, for $\omega = 30°$ and 45°, respectively), the ratio K_{IC}/K_{IC}^{br} decreases with increasing grain size. This implies that the enhancing effect of the examined deformation mechanism on the critical stress intensity factor K_{IC} (characterizing fracture toughness of nanocrystalline solids) is especially pronounced for small grain sizes. This is in contrast to the situation with lattice dislocation emission from crack tips – the conventional toughening mechanism in metallic materials – whose enhancing effect on the fracture toughness of nanocrystalline metals rapidly decreases with a decrease in grain size [46].

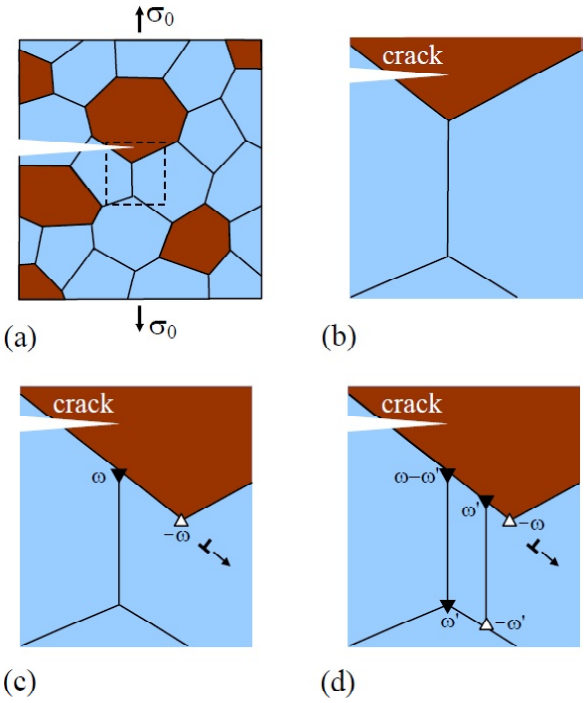

Fig. 4. Grain boundary deformation processes in nanocrystalline metal-ceramic composites near a crack tip. (a) General view. Metallic and ceramic grains are schematically shown as blue and brown polygons, respectively. (b) Initial configuration I of grain boundaries. (c) Configuration II results from pure grain boundary sliding. (d) Configuration III results from cooperative grain boundary sliding and nanograin nucleation process.

4. CONCLUDING REMARKS

Thus, the results of our calculations show that cooperative sliding along a single GB and nanograin nucleation can make the critical stress intensity factor K_{IC} several times larger. Apparently, cooperative GB nanograin nucleation and sliding along various GBs can increase the value of K_{IC} further and, as a result, may lead to a significant improvement of fracture toughness, as compared to the case of pure brittle fracture. For example, if one supposes that cooperative GB migration and sliding can increase the value of K_{IC} by a factor of 6 (as compared to the case of pure brittle intragrain fracture), they would obtain: $K_{IC} = 6K_{IC}^{br} \approx 5.33$ MPa·m$^{1/2}$ in the case of nanocrystalline Ni. The obtained value of K_{IC} for nanocrystalline Ni is still much smaller than typical values of K_{IC} for polycrystalline Ni, which are as large as several tens of MPa·m$^{1/2}$. However, in

combination with other toughening mechanisms (limited dislocation emission from crack tips, stress-driven GB migration, diffusion, etc.), the suggested mechanism of cooperative GB sliding and nanograin nucleation can result in good fracture toughness of nanocrystalline materials, documented in several experiments (e.g., [27–30]).

Finally, note that the suggested theoretical model is relevant to the description of the effect caused by the CGBSNN process on fracture toughness of metallic and ceramic NMs as well as metal-ceramic nanocrystalline composites (Fig. 4). In the latter case, GB sliding (as a constituent of the CGBSNN process) can occur along metal/metal, metal/ceramic and/or ceramic/ceramic interfaces, depending on both their resistivity to this sliding and stress levels near crack tips, and GB migration (as a constituent of the CGBSNN process) can occur in metallic and/or ceramic grains. This variety of constituent processes of the CGBSNN provides its flexibility and enhancement in metal-ceramic nanocrystalline composites.

ACKNOWLEDGEMENT

This work was supported by the Russian Science Foundation (Research Project 14-29-00199).

REFERENCES

[1] L. Lu, M. L. Sui and K. Lu // *Science* **287** (2000) 1463.
[2] M. Chen, E. Ma, K.J. Hemker, H. Sheng, Y.M. Wang and X. Cheng // *Science* **300** (2003) 1275.
[3] M.Yu. Gutkin, I.A. Ovid'ko and N.V. Skiba // *Mater. Sci. Eng.* A **339** (2003) 73.
[4] W.A. Soer, J.T.M. De Hosson, A.M. Minor, J.W. Morris, Jr. and E.A. Stach // *Acta Mater*. **52** (2004) 5783.
[5] S.V. Bobylev, M.Yu. Gutkin and I.A. Ovid'ko // *Phys. Rev.* B **73** (2006) 054102.
[6] D.S. Gianola, S. Van Petegem, M. Legros, S. Brandstetter, H. Van Swygenhoven and K.J. Hemker // *Acta Mater.* **54** (2006) 2253.
[7] F. Sansoz and V. Dupont // *Appl. Phys. Lett.* **89** (2006) 111901.
[8] A.S. Khan, B. Farrok and L. Takacs // *J. Mater. Sci.* **43** (2008) 3305.
[9] S. Cheng, Y. Zhao, Y. Wang, Y. Li, X.-L. Wang, P.K. Liaw and E.J. Lavernia // *Phys. Rev. Lett.* **104 (2010)** 255501.
[10] Y.M. Wang, R.T. Ott, A.V. Hamza, M.F. Besser, J. Almer and M.J. Kramer // *Phys. Rev. Lett.* **105** (2010) 215502.
[11] J. Lohmiller, A. Kobler, R. Spolenak and P.A. Gruber // *Appl. Phys. Lett.* **102** (2013) 241916.
[12] Y.-B. Guo, T. Xu and M. Li // *Appl. Phys. Lett.* **102** (2013) 241910.
[13] S. Cheng, S.Y. Lee, L. Li, C. Lei, J. Almer, X.-L. Wang, T. Ungar, Y. Wang and P.K. Liaw // *Phys. Rev. Lett.* **110** (2013) 135501.
[14] X. Yu, Y. Wang, J. Zhang, H. Xu and Y. Zhao // *Appl. Phys. Lett.* **103** (2013) 043118.
[15] G. Liu, G.J. Zhang, F. Jiang, X.D. Ding, Y.J. Sun and E. Ma // *Nature Mater*. **12** (2013) 344.
[16] J. Li, A. K. Soh and X. Wu // *Scr. Mater*. **78-79** (2014) 5.
[17] J.D. Kuntz, G.-D. Zhan and A.K. Mukherjee // *MRS Bullet.* **29** (2004) 22.
[18] M. Dao, L. Lu, R.J. Asaro, J.T.M. De Hosson and E. Ma // *Acta Mater.* **55** (2007) 4041.
[19] A. Mukhopadhyay and B. Basu // *Int. Mater. Rev.* **52** (2007) 257.
[20] M. Kawasaki and T.G. Langdon // *J. Mater. Sci.* **42** (2007) 1782.
[21] C.S. Pande and K.P. Cooper // *Progr. Mater. Sci.* **54** (2009) 689.
[22] H.A. Padilla II and B.L. Boyce // *Exp. Mechanics* **50** (2010) 5.
[23] I.A. Ovid'ko and T.G. Langdon // *Rev. Adv. Mater. Sci*. **30** (2012) 103.
[24] S. Cheng, E. Ma, Y.M. Wang, L.J. Kecskes, K.M. Youssef, C.C. Koch, U.P. Trociewitz and K. Han // *Acta Mater.* **53** (2005) 1521.
[25] K.M. Youssef, R.O. Scattergood, K.L. Murty, J.A. Horton and C.C. Koch // *Appl. Phys. Lett.* **87** (2005) 091904.
[26] K.M. Youssef, R.O. Scattergood, K.L. Murty and C.C. Koch // *Scripta Mater.* **54** (2006) 251.
[27] A.V. Sergueeva, N.A. Mara and A.K. Mukherjee // *J. Mater. Sci.* **42** (2007) 1433.
[28] R.A. Mirshams, C.H. Liao, S.H. Wang and W.M. Yin // *Mater. Sci. Eng.* A **315** (2001) 21.
[29] Y. Zhao, J. Qian, L.L. Daemen, C. Pantea, J. Zhang, G.A. Voronin and T.W. Zerda // *Appl. Phys. Lett.* **84** (2004) 1356.
[30] A.A. Kaminskii, M.S. Akchurin, R.V. Gainutdinov, K. Takaichi, A. Shirakava, H. Yagi, T. Yanagitani and K. Ueda // *Crystall. Rep.* **50** (2005) 869.
[31] Y.T. Pei, D. Galvan and J.T.M. De Hosson // *Acta Mater.* **53** (2005) 4505.
[32] I.A. Ovid'ko and A.G. Sheinerman // *Rev. Adv. Mater. Sci*. **29** (2011) 105.

[33] S.V. Bobylev, A.K. Mukherjee, I.A. Ovid'ko and A.G. Sheinerman // *Int. J. Plasticity* **26** (2010) 1629.
[34] S.V. Bobylev, N.F. Morozov and I.A. Ovid'ko // *Phys. Rev. Lett.* **105** (2010) 055504.
[35] S.V. Bobylev, N.F. Morozov and I.A. Ovid'ko // *Phys. Rev.* B **84** (2011) 094103.
[36] I.A. Ovid'ko, A.G. Sheinerman and E.C. Aifantis // *Acta Mater.* **59** (2011) 5023.
[37] I.A. Ovid'ko and A.G. Sheinerman // *Appl. Phys. Lett.* **90** (2007) 171927.
[38] I.A. Ovid'ko and A.G. Sheinerman // *Acta Mater.* **57** (2009) 2217.
[39] S.V. Bobylev and I.A.Ovidko // *Appl. Phys. Lett.* **92** (2008) 081914.
[40] S.V. Bobylev and I.A.Ovidko // *Rev. Adv. Mater. Sci*. **17** (2008) 76.
[41] N.F. Morozov, I.A. Ovid'ko, A.G. Sheinerman and E.C. Aifantis // *J. Mech. Phys. Solids* **58** (2010) 1088.
[42] V.M. Kuznetsov, R.I. Kadyrov and G.E. Rudenskii // *J. Mater. Sci. Technol.* **14** (1998) 320.
[43] R.G. Irwin // *J. Appl. Mech.* **24** (1957) 361.
[44] *Fracture Mechanics and Strength of Materials*, ed. by V.V. Panasyuk (Naukova Dumka, Kiev, 1988). Vol. 2 (in Russian).
[45] J.P. Hirth and J. Lothe, *Theory of Dislocations* (Wiley, New York, 1982).
[46] I.A. Ovid'ko and A.G. Sheinerman // *Acta Mater.* **58** (2010) 5286.